Title

Engineer P. multocida Heparosan Synthase 2 (PmHS2) for Size-Controlled Synthesis of Longer Heparosan Oligosaccharides

Journal

ACS Catalysis, 10(11)

ISSN

2155-5435

Authors

Na, Lan
Yu, Hai
McArthur, John B
et al.

Publication Date

2020-06-05

DOI

10.1021/acscatal.0c01231

Peer reviewed

Published in final edited form as:

ACS Catal. 2020 June 5; 10(11): 6113–6118. doi:10.1021/acscatal.0c01231.

Engineer *P. multocida* Heparosan Synthase 2 (PmHS2) for Size-Controlled Synthesis of Longer Heparosan Oligosaccharides

Lan Na[†], **Hai Yu**[†,*], **John B. McArthur**, **Tamashree Ghosh**, **Thomas Asbell**, **Xi Chen**[*]

Department of Chemistry, University of California, One Shields Avenue, Davis, California 95616, United States

Abstract

Pasteurella multocida heparosan synthase 2 (PmHS2) is a dual-function polysaccharide synthase having both α1–4-N-acetylglucosaminyltransferase (α1–4-GlcNAcT) and β1–4-glucuronyltransferase (β1–4-GlcAT) activities located in two separate catalytic domains. We found that removing PmHS2 N-terminal 80-amino acid residues improved enzyme stability and expression level while retaining its substrate promiscuity. We also identified the reverse glycosylation activities of PmHS2 which complicated its application in size-controlled synthesis of oligosaccharides longer than hexasaccharide. Engineered Δ80PmHS2 single-function-glycosyltransferase mutants Δ80PmHS2_D291N (α1–4-GlcNAcT lacking both forward and reverse β1–4-GlcAT activities) and Δ80PmHS2_D569N (β1–4-GlcAT lacking both forward and reverse α1–4-GlcNAcT activities) were designed and showed to minimize side product formation. They were successfully used in a sequential one-pot multienzyme (OPME) platform for size-controlled high-yield production of oligosaccharides up to decasaccharide. The study draws attention to the consideration of reverse glycosylation activities of glycosyltransferases, including polysaccharide synthases, when applying them in the synthesis of oligosaccharides and polysaccharides. The mutagenesis strategy has the potential to be extended to other multifunctional polysaccharide synthases with reverse glycosylation activities to generate catalysts with improved synthetic efficiency.

Graphical Abstract

[*]**Corresponding Authors:** xiichen@ucdavis.edu; hyu@ucdavis.edu.

[†]Author Contributions

These authors contributed similarly to this work.

The authors declare no competing financial interest.

ASSOCIATED CONTENT

Supporting Information.

This material is available free of charge via the Internet at http://pubs.acs.org.

Supporting figures and experimental details for cloning and characterization of Δ80PmHS2 and mutants; detailed synthetic procedures, nuclear magnetic resonance (NMR) spectroscopy and high-resolution mass spectrometry (HRMS) data, and NMR spectra of products (PDF)

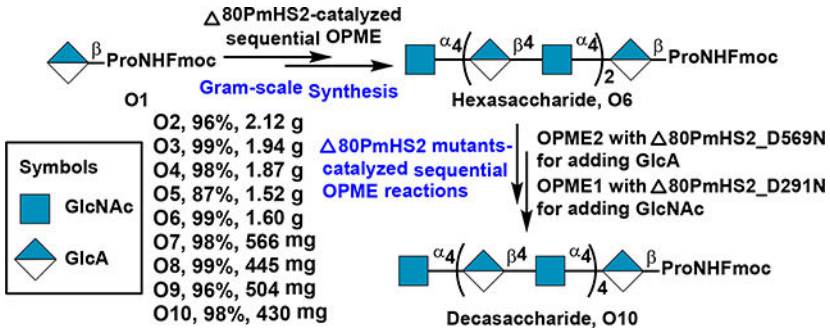

Keywords

biocatalysis; bacterial polysaccharide; carbohydrate; chemoenzymatic synthesis; glycosaminoglycan

Heparin (HP) and heparan sulfate (HS) glycosaminoglycans (GAGs) are structurally complex, sulfated linear polysaccharides known to bind to over 300 different human proteins.[1] They are biosynthesized from heparosan, which is a polysaccharide backbone containing a −4GlcNAcα1–4GlcAβ1- disaccharide repeat, followed by orchestrated functions of a group of carbohydrate post-glycosylational modification (PGM) enzymes to produce diverse sulfation and epimerization patterns.[2–3] HP is a clinically used anticoagulant while both HP and HS may have broader potential applications including cancer treatment and protection against virus infections.[4–5] Due to their structure complexity, detailed structure-activity relationships of HP and HS remain unclear.[6–7] Structurally defined synthetic compounds will provide invaluable standards and probes to better understand their important roles and accelerate their applications.

Despite much progress,[8–12] the process for chemical synthesis of HS and HP oligosaccharides is still tedious and challenging especially for longer structure targets. Chemoenzymatic methods are powerful alternatives.[13–18] Glycosyltransferases and polysaccharide synthases involved in the production of heparosan-based capsular polysaccharides have been identified from pathogenic bacteria *Escherichia coli* K5,[19] *Pasteurella multocida* Type D (PmHS1),[20] and *Avibacterium paragallinarum* genotype II.[21] *Pasteurella multocida* heparosan synthase 2 (PmHS2) which was not part of bacterial capsule biosynthesis loci has been discovered in *Pasteurella multocida* type A, D, and F strains.[22] Both PmHS1[20] and PmHS2[22] are dual function polysaccharide synthases having both α1–4-N-acetylglucosaminyltransferase (α1–4-GlcNAcT) and β1–4-glucuronyltransferase (β1–4-GlcAT) activities contributed by two separate catalytic domains[14] similar to the case in PmHS1.[14, 23] Compared to PmHS1, PmHS2 has higher expression levels in *E. coli*, no requirement for an oligosaccharide primer, and a higher substrate promiscuity.[24] PmHS2 has been used broadly in enzymatic synthesis of heparosan polysaccharides,[14–15] and in chemoenzymatic synthesis of HP and HS oligosaccharides and their derivatives with[16–17] or without[18] *Escherichia coli* K5 α1–4-GlcNAcT (EcKfiA).

Nevertheless, the expression level (17–20 mg/L culture) and the stability of PmHS2[18] can be improved. Additionally, PmHS2 was efficient in synthesizing short oligosaccharides up to

hexasaccharides[25] but longer glycans were obtained in lower yields (e.g. 35% yield for a decasaccharide).[17] On the other hand, longer HS oligosaccharides (e.g. octasaccharides–dodecasaccharide) were required for strong interaction with some HP-binding proteins.[26–29] For example, decasaccharide was found to be minimum for efficient binding of bone morphogenetic protein-2 (BMP-2).[30] We planned to engineer PmHS2 to improve its application in size-controlled chemoenzymatic synthesis of heparosan, HS, HP oligosaccharides and derivatives.

Analyzing PmHS2 protein sequence using XtalPredRF[31] (Figure S1A) and BLAST (Figure S1B) predicted that its N-terminal 80 amino acid residues might be nonessential to its glycosyltransferase activities and unfavorable for its crystallizability and stability. Indeed, removing the N-terminal 80 amino acid residues of PmHS2 (Figure S2) (17–20 mg/L culture) resulted in Δ80PmHS2 (Figure S3) (60–80 mg/L) with a 3–4-fold improved expression level (Figure S4) and an improved thermal stability (Figure S5). In contrast to PmHS2 which precipitated easily during dialysis, Δ80PmHS2 remained soluble. Δ80PmHS2 could also survive lyophilization without loss of activity (Figure S6). On the other hand, Δ80PmHS2 (pI 6.61) and PmHS2[32] (pI 6.83) share similar pH profiles (Figure S7) and donor substrate promiscuities (Figure S8). A previously synthesized stable GlcAβ2AA[18] was used as a fluorescent-labeled acceptor substrate in these assays to allow easy product detection by high-performance liquid chromatography (HPLC) with a diode array or UV/Vis detector.

To facilitate reaction monitoring, product purification, and allow easy removal from the products for downstream conjugation with proteins or other molecules, a fluorophore tag was introduced to two possible monosaccharide substrates. GlcAβProNHFmoc (**O1**) and GlcNAcαProNHFmoc were synthesized from the corresponding glycosylpropylazides GlcAβProN_3[18] and GlcNAcαProN_3[33] by catalytic hydrogenation followed by coupling with *N*-(9-fluorenylmethoxycarbonyloxy)succinimide (Fmoc-Suc) (see ESI).

Activity comparison (Table S1) showed that GlcAβProNHFmoc (**O1**) was a more efficient substrate than GlcNAcαProNHFmoc for both PmHS2 (157-fold) and Δ80PmHS2 (130-fold) in disaccharide production. Apparent kinetics studies with GlcAβ2AA (Table S2) showed that PmHS2 (3.4±0.2 s^{-1}) and Δ80PmHS2 (3.5±0.2 s^{-1}) have similar k_{cat} values while PmHS2 (4.0±0.6 mM) has a lower K_M value than Δ80PmHS2 (5.3±0.7 mM), resulting in a slightly higher catalytic efficiency for PmHS2 (0.9 s^{-1} mM^{-1}) than Δ80PmHS2 (0.7 s^{-1} mM^{-1}).

Starting from GlcAβProNHFmoc (**O1**), Δ80PmHS2 with improved expression and stability permitted size-controlled gram-scale synthesis of heparosan oligosaccharides ranging from disaccharide (**O2**) to hexasaccharide (**O6**) in excellent yields using a sequential one-pot multienzyme (OPME) platform. In this platform (Scheme 1), GlcNAc-activation/transfer (**OPME1**) and GlcA-activation/transfer (**OPME2**) systems (each contains Δ80PmHS2, a kinase, a nucleotidyltransferase, and an inorganic pyrophosphatase) were used alternately to extend the acceptor substrate chain one monosaccharide at a time. Each OPME reaction was carried out for 1–2 days, the product was purified and used as the acceptor substrate for the next OPME reaction.

As shown in Scheme 1, disaccharide GlcNAcα1–4GlcAβProNHFmoc (**O2**) was enzymatically synthesized from **O1** using a one-pot four-enzyme GlcNAc-activation and transfer system (**OPME1**) containing *Bifidobacterium longum* N-acetylhexosamine-1-kinase (BLNahK),[34] *Pasteurella multocida N*-acetylglucosamine-1-phosphate uridylyltransferase (PmGlmU),[35] *Pasteurella multocida* inorganic pyrophosphatase (PmPpA),[33] and Δ80PmHS2. The reaction went to completion and the product was readily purified by passing the reaction mixture through a C18 cartridge and eluting with a gradient solution of CH_3CN in water. Purified disaccharide **O2** (2.12 g) was obtained in an excellent 96% yield. Trisaccharide GlcAβ1–4GlcNAcα1–4GlcAβProNHFmoc (**O3**) (1.94 g) was synthesized from purified disaccharide **O2** using a one-pot four-enzyme GlcA-activation and transfer system (**OPME2**) containing *Arabidopsis thaliana* glucuronokinase (AtGlcAK),[36] *Bifidobacterium longum* UDP-sugar pyrophosphorylase (BLUSP),[37] PmPpA, and Δ80PmHS2 with a purified yield of 99%. Repeating the alternate **OPME1** and **OPME2** reactions with C18-cartridge-based product purification after each OPME reaction led to the formation of tetrasaccharide **O4** (1.87 g, 98%), pentasaccharide **O5** (1.52 g, 87%), and hexasaccharide **O6** (1.60 g, 99%).

OPME reactions of GlcNAc activation and transfer to glucuronides **O1**, **O3**, and **O5** (**OPME1**) were highly efficient and *N*-acetylglucosaminides **O2**, **O4**, and **O6** were obtained in nearly quantitative yields (96–99%). In the case of OPME reactions of GlcA activation and transfer to *N*-acetylglucosaminides **O2** and **O4** (**OPME2**) for the formation of glucuronides **O3** and **O5**, the reaction with **O2** went well and **O3** was obtained in an excellent 99% yield. However, when tetrasaccharide **O4** (an *N*-acetylglucosaminide longer than **O2**) was used as an acceptor for the formation of **O5**, the presence of **O3** byproduct was observed, indicating that the terminal GlcNAc in the acceptor **O4** was removed in the reaction. The side product formation was minimized by monitoring the reaction progress carefully and stopping the reaction promptly to obtain **O5** in 87% yield.

Overall, the sequential OPME platform containing Δ80PmHS2 was efficient in gram-scale synthesis of heparosan oligosaccharides up to hexasaccharide **O6** from monosaccharide **O1**. When hexasaccharide **O6** (an *N*-acetylglucosaminide even longer than **O4**) was used as the acceptor substrate for the β1–4-GlcAT activity of Δ80PmHS2, the formation of both longer and shorter oligosaccharide byproducts (Figure S9) was observed, which complicated product purification and lowered synthetic yields.

We hypothesized that the formation of longer and shorter oligosaccharide byproducts in the OPME reaction for the synthesis of **O7** from **O6** was due to the reverse glycosylation activity of Δ80PmHS2. Such activity was reported for some glycosyltransferases involved in natural product glycosylation,[38–39] mammalian sialyltransferases,[40] and bacterial sialyltransferases *Pasteurella multocida* sialyltransferase 1 (PmST1) and *Photobacterium damselae* α2–6-sialyltransferase (Pd2,6ST),[41–42] but was not observed for others.[40] Such activity, however, has never been shown for polysaccharide synthases. To test the hypothesis, hexasaccharide **O6** was incubated with Δ80PmHS2 in the absence or the presence of different concentrations of uridine 5’-diphosphate (UDP). As shown in Table S3, the amounts of Δ80PmHS2 reverse glycosylation products (oligosaccharides of various sizes

ranging from mono- to dodecasaccharide) increased and the concentration of **O6** decreased significantly with the increase of UDP concentration. The same effects were observed for PmHS2 (Table S3), demonstrating that the reverse glycosylation property was not introduced by the N-terminal protein sequence truncation in Δ80PmHS2. The chain reactions caused by the forward and reverse glycosylation reactions of Δ80PmHS2 in the presence of **O6** and UDP are illustrated in Scheme 2. Starting from **O6**, the reverse α1–4-GlcNAcT activity of Δ80PmHS2 produces **O5** and UDP-GlcNAc. The resulting **O5** is used by the reverse β1–4-GlcAT activity of Δ80PmHS2 to produce **O4** and UDP-GlcA. On the other hand, the UDP-GlcA obtained is used together with **O6** by the β1–4-GlcAT activity of Δ80PmHS2 to produce **O7** and UDP. The α1–4-GlcNAcT activity of Δ80PmHS2 uses **O7** and UDP-GlcNAc to produce **O8** and UDP. Similarly, the newly formed longer and shorter oligosaccharides in the reaction mixture are used as the substrates in combined Δ80PmHS2-catalyzed forward and reverse glycosylation reactions for the formation of additional oligosaccharides of longer and shorter lengths.

Time course studies using GlcNAc-terminated **O6** as the substrate for Δ80PmHS2 (Figure S10) showed that longer incubation times led to a continuous decrease of **O6** concentration and increased dispersity of oligosaccharide products with a preference toward the accumulation of GlcNAc-terminated oligosaccharides (**O2**, **O4**, **O8**, and **O10**). The production of oligosaccharides of different sizes indicated that both α1–4-GlcNAcT and β1–4-GlcAT activities of Δ80PmHS2 have the corresponding reverse glycosylation activities. Indeed, incubating Δ80PmHS2 with GlcA-terminated pentasaccharide **O5** in the presence of UDP (Figure S11) also showed a time-dependent increase of the product dispersity although GlcA-terminated oligosaccharide products (**O3**, **O7**, and **O9**) dominated. Increased product dispersity with the increase of time was also observed previously in PmHS2-catalyzed polymerization reactions,[15, 43] although reverse glycosylation was not realized as a likely major contributor.

The formation of UDP-GlcNAc by reverse glycosylation of **O6** using Δ80PmHS2 in the presence of UDP was further confirmed by a coupled enzyme assay (Scheme 3) inspired by Mehr et al. for indirectly detecting CMP-sialic acid formed in a reverse-sialyltransferase reaction.[41] To do this, an additional glycosyltransferase *Neisseria meningitidis* β1–3-N-acetylglucosaminyltransferase (NmLgtA)[44] and its acceptor 4-methylumberliferyl β-lactoside (LacβMU)[45] were added to the reaction of Δ80PmHS2 in the presence of **O6** and UDP. As expected (Table S4), GlcNAcβ1–3LacβMU formed by NmLgtA-catalyzed reaction was observed only in the reaction containing all components including NmLgtA, Δ80PmHS2, and UDP (**Reaction 1** in Table S4) but not in the one lacking NmLgtA (**Reaction 2** in Table S4), Δ80PmHS2 (**Reaction 3** in Table S4), or UDP (**Reaction 4** in Table S4).

Since reverse α1–4-GlcNAcT and β1–4-GlcAT activities of Δ80PmHS2 cause challenges in size-controlled enzymatic synthesis and purification of longer oligosaccharide products, mutagenesis studies of Δ80PmHS2 were planned to generate single-function glycosyltransferases by mutating the key catalytic base residues of the other glycosyltransferase domains. The previously reported strategy of generating single-functional glycosyltransferases of PmHS2[14] and PmHS1[23] by mutating the

glycosyltransferase DXD motifs was not adopted due to the significant decrease of the stability of the PmHS2 mutants[14] which would adversely affect their application in synthesis. In the absence of known PmHS2 crystal structures, a Δ80PmHS2 I-TASSER[46–47] model was generated. The β1–4-GlcAT domain in Δ80PmHS2 I-TASSER model aligned well with the GalNAcT and GlcAT domains of *Escherichia coli* K4 chondroitin polymerase (EcKfoC) (PDB ID: 2Z86 and 2Z87)[48] (Figure S12), identifying D291 as a possible catalytic base. Similarly, a potential key catalytic residue (D569) in the Δ80PmHS2 α1–4-GlcNAcT domain was identified by aligning its I-TASSER model with the structures of *Neisseria meningitidis* lipopolysaccharyl-α1,4-galactosyltransferase (NmLgtC)[49–51] and bovine α1–3-galactosyltransferase (α3GalT)[52] (Figure S13).

D291N and D569N mutants of Δ80PmHS2 were generated (Figure S14). Their expression levels (50–60 and 60–70 mg/L culture, respectively) were comparable to that of Δ80PmHS2 (60–80 mg/L culture). The D291N mutant retained the α1–4-GlcNAcT activity and lost the β1–4-GlcAT activity of Δ80PmHS2. In contrast, the D569N mutant retained Δ80PmHS2 β1–4-GlcAT activity while its α1–4-GlcNAcT activity decreased 548-fold (Figure S15). The corresponding reverse glycosylation activities of Δ80PmHS2 also decreased significantly in the mutants. As shown in Figure S16, under conditions mimicking synthetic reactions with 30 mM UDP (Figures S16A–B), no reverse glycosylation oligosaccharide products were observed for either mutants, demonstrating the efficiency of the mutants in blocking the cascade chain reactions shown in Scheme 2 and avoiding the generation of multiple oligosaccharide byproducts.

Δ80PmHS2_D569N mutant was used as a single function β1–4-GlcAT (lacking both forward and reverse α1–4-GlcNAcT activities) in high-yield OPME synthesis (**OPME2**) (Scheme 4) of longer GlcA-terminated heparosan oligosaccharides including heptasaccharide **O7** (566 mg, 98%) and nonasaccharide **O9** (445 mg, 96%), respectively, from the corresponding GlcNAc-terminated Δ80PmHS2_D569N oligosaccharide acceptors **O6** and **O8**. Δ80PmHS2_D291N mutant was used as a single function α1–4-GlcNAcT (lacking both forward and reverse β1–4-GlcAT activities) for high-yield OPME (**OPME1**) synthesis of longer GlcNAc-terminated oligosaccharides including octasaccharide **O8** (504 mg, 99%) and decasaccharide **O10** (430 mg, 98%), respectively, from the corresponding GlcA-terminated Δ80PmHS2_D291N oligosaccharide acceptors **O7** and **O9**. In these preparative-scale OPME reactions, unwanted oligosaccharide byproducts were not observed.

Various NMR experiments for **O1**–**O10** including ^{1}H and ^{13}C NMR, HSQC, and HSQC-TOCSY (90 ms and 10 ms) enabled signal assignments and the observation of key correlations. HSQC spectra provided C−H coupling information, and HSQC-TOCSY with 90 ms and 10 ms mixing times indicated independent coupling correlations of terminal and internal GlcA or GlcNAc residues. In the example of **O3** containing two GlcA residues, the chemical shifts of the internal GlcA are more downfield for H3 (differ by 0.30 ppm), H4 (differ by 0.17 ppm), H5 (differ by 0.07 ppm), C1 (differ by 0.11 ppm), C2 (differ by 0.73 ppm), C3 (differ by 0.34 ppm), C4 (differ by 4.95 ppm), and C5 (differ by 3.18 ppm), but more upfield for H-1 (differ by 0.18 ppm) than that of the terminal GlcA.

In conclusion, N-terminal truncated Δ80PmHS2 with improved expression level and stability was shown to be an efficient catalyst for gram-scale sequential OPME synthesis of heparosan oligosaccharides up to hexasaccharide **O6**. Reverse glycosylation activities of Δ80PmHS2 were characterized and shown to be responsible for poor yields and complications in Δ80PmHS2-involved OPME synthesis of longer oligosaccharides. Key catalytic base residues for the β1–4-GlcAT and the α1–4-GlcNAcT activities of Δ80PmHS2 were identified. Δ80PmHS2_D569N and Δ80PmHS2_D291N mutants were generated as single functional β1–4-GlcAT and α1–4-GlcNAcT with significantly decreased reverse α1–4-GlcNAcT and reverse β1–4-GlcAT glycosyltransferase activities, respectively. They have been used as efficient catalysts for sequential OPME synthesis of longer length heparosan oligosaccharides (**O7**–**O10**). The study draws attention to the consideration of reverse glycosylation activities of glycosyltransferases including polysaccharide synthases when applying them in the synthesis of oligosaccharides and polysaccharides. The mutagenesis strategy has the potential to be extended to other multifunctional polysaccharide synthases with reverse glycosylation activities, especially those use sugar nucleotides containing the same nucleotide component, to generate catalysts with improved synthetic efficiency.

Supplementary Material

Refer to Web version on PubMed Central for supplementary material.

ACKNOWLEDGMENT

This work was supported by the United States National Institutes of Health (NIH) Common Fund for Glycoscience Program grant U01GM125288 and NIH grant R01GM094523. Bruker Avance-800 NMR spectrometer was funded by NSF grant DBI-0722538.

REFERENCES

(1). Xu D; Esko JD Demystifying Heparan Sulfate-Protein Interactions. Annu. Rev. Biochem. 2014, 83, 129–257. [PubMed: 24606135]

(2). Lindahl U; Couchman J; Kimata K; Esko JD Proteoglycans And Sulfated Glycosaminoglycans In Essentials of Glycobiology, 3rd Ed.; Varki A; Cummings RD; Esko JD; Stanley P; Hart GW; Aebi M; Darvill AG; Kinoshita T; Packer NH; Prestegard JH; Schnaar RL; Seeberger PH Eds. Cold Spring Harbor (NY), 2015; pp 207–221.rd

(3). Yu H; Chen X Carbohydrate Post-Glycosylational Modifications. Org. Biomol. Chem. 2007, 5, 865–872. [PubMed: 17340000]

(4). Chavaroche AA; van den Broek LA; Eggink G Production Methods for Heparosan, A Precursor of Heparin And Heparan Sulfate. Carbohydr. Polym. 2013, 93, 38–47. [PubMed: 23465899]

(5). Li P; Sheng J; Liu Y; Li J; Liu J; Wang F Heparosan-Derived Heparan Sulfate/Heparin-Like Compounds: One Kind of Potential Therapeutic Agents. Med. Res. Rev. 2013, 33, 665–692. [PubMed: 22495734]

(6). Lanzi C; Cassinelli G Heparan Sulfate Mimetics in Cancer Therapy: The Challenge to Define Structural Determinants and the Relevance of Targets for Optimal Activity. Molecules 2018, 23, 2915.

(7). Maciej-Hulme ML; Skidmore MA; Price HP The Role of Heparan Sulfate in Host Macrophage Infection by Leishmania species. Biochem Soc Trans 2018, 46, 789–796. [PubMed: 29934302]

(8). Sinaÿ P; Jacquinet J-C; Petitou M; Duchaussoy P; Lederman I; Choay J; Torri G Total Synthesis of A Heparin Pentasaccharide Fragment Having High Affinity for Antithrombin III. Carbohydr. Res. 1984, 132, C5–C9.

(9). Zong C; Venot A; Li X; Lu W; Xiao W; Wilkes JL; Salanga CL; Handel TM; Wang L; Wolfert MA; Boons GJ Heparan Sulfate Microarray Reveals That Heparan Sulfate-Protein Binding Exhibits Different Ligand Requirements. J. Am. Chem. Soc. 2017, 139, 9534–9543. [PubMed: 28651046]

(10). Hung SC; Lu XA; Lee JC; Chang MD; Fang SL; Fan TC; Zulueta MM; Zhong YQ Synthesis of Heparin Oligosaccharides And Their Interaction with Eosinophil-Derived Neurotoxin. Org. Biomol. Chem. 2012, 10, 760–772. [PubMed: 22143347]

(11). Huang TY; Irene D; Zulueta MM; Tai TJ; Lain SH; Cheng CP; Tsai PX; Lin SY; Chen ZG; Ku CC; Hsiao CD; Chyan CL; Hung SC Structure of The Complex Between A Heparan Sulfate Octasaccharide And Mycobacterial Heparin-Binding Hemagglutinin. Angew. Chem., Int. Ed. 2017, 56, 4192–4196.

(12). Hu Y-P; Lin S-Y; Huang C-Y; Zulueta MML; Liu J-Y; Chang W; Hung S-C Synthesis of 3-O-Sulfonated Heparan Sulfate Octasaccharides That Inhibit The Herpes Simplex Virus Type 1 Host–Cell Interaction. Nat. Chem. 2011, 3, 557–563. [PubMed: 21697878]

(13). Liu J; Linhardt RJ Chemoenzymatic Synthesis of Heparan Sulfate And Heparin. Nat. Prod. Rep. 2014, 31, 1676–1685. [PubMed: 25197032]

(14). Chavaroche AA; van den Broek LA; Springer J; Boeriu C; Eggink G Analysis of The Polymerization Initiation And Activity of *Pasteurella multocida* Heparosan Synthase PmHS2, An Enzyme with Glycosyltransferase And UDP-Sugar Hydrolase activity. J. Biol. Chem. 2011, 286, 1777–1785. [PubMed: 21084307]

(15). Chavaroche AA; Springer J; Kooy F; Boeriu C; Eggink G *In vitro* Synthesis of Heparosan Using Recombinant *Pasteurella multocida* Heparosan Synthase PmHS2. Appl. Microbiol. Biotechnol. 2010, 85, 1881–1891. [PubMed: 19756580]

(16). Xu Y; Masuko S; Takieddin M; Xu H; Liu R; Jing J; Mousa SA; Linhardt RJ; Liu J Chemoenzymatic Synthesis of Homogeneous Ultralow Molecular Weight Heparins. Science 2011, 334, 498–501. [PubMed: 22034431]

(17). Liu R; Xu Y; Chen M; Weiwer M; Zhou X; Bridges AS; DeAngelis PL; Zhang Q; Linhardt RJ; Liu J Chemoenzymatic Design of Heparan Sulfate Oligosaccharides. J. Biol. Chem. 2010, 285, 34240–34249. [PubMed: 20729556]

(18). Chen Y; Li Y; Yu H; Sugiarto G; Thon V; Hwang J; Ding L; Hie L; Chen X Tailored Design and Synthesis of Heparan Sulfate Oligosaccharide Analogues Using Sequential One-Pot Multienzyme Systems. Angew. Chem., Int. Ed.. 2013, 52, 11852–11856.

(19). Vann WF; Schmidt MA; Jann B; Jann K The Structure of The Capsular Polysaccharide (K5 Antigen) of Urinary-Tract-Infective Escherichia coli 010:K5:H4. A Polymer Similar to Desulfo-Heparin. Eur. J. Biochem. 1981, 116, 359–364. [PubMed: 7018909]

(20). DeAngelis PL; White CL Identification And Molecular Cloning of A Heparosan Synthase from *Pasteurella multocida* Type D. J. Biol. Chem. 2002, 277, 7209–7213. [PubMed: 11756462]

(21). Wu JR; Chen PY; Shien JH; Shyu CL; Shieh HK; Chang F; Chang PC Analysis of The Biosynthesis Genes And Chemical Components of The Capsule of *Avibacterium paragallinarum*. Vet. Microbiol. 2010, 145, 90–99. [PubMed: 20362405]

(22). DeAngelis PL; White CL Identification of A Distinct, Cryptic Heparosan Synthase from *Pasteurella multocida* Types A, D, and F. J. Bacteriol. 2004, 186, 8529–8532. [PubMed: 15576804]

(23). Kane TA; White CL; DeAngelis PL, Functional Characterization of PmHS1, A *Pasteurella multocida* Heparosan Synthase. J. Biol. Chem. 2006, 281, 33192–33197. [PubMed: 16959770]

(24). Sismey-Ragatz AE; Green DE; Otto NJ; Rejzek M; Field RA; DeAngelis PL Chemoenzymatic Synthesis with Distinct *Pasteurella heparosan* Synthases: Monodisperse Polymers And Unnatural Structures. J. Biol. Chem. 2007, 282, 28321–28327. [PubMed: 17627940]

(25). Wu B; Wei N; Thon V; Wei M; Yu Z; Xu Y; Chen X; Liu J; Wang PG; Li T Facile Chemoenzymatic Synthesis of Biotinylated Heparosan Hexasaccharide. Org. Biomol. Chem. 2015, 13, 5098–5101. [PubMed: 25858766]

(26). DiGabriele AD; Lax I; Chen DI; Svahn CM; Jaye M; Schlessinger J; Hendrickson WA Structure of A Heparin-Linked Biologically Active Dimer of Fibroblast Growth Factor. Nature 1998, 393, 812–817. [PubMed: 9655399]

(27). Xu D; Young JH; Krahn JM; Song D; Corbett KD; Chazin WJ; Pedersen LC; Esko JD Stable RAGE-Heparan Sulfate Complexes Are Essential for Signal Transduction. ACS Chem. Biol. 2013, 8, 1611–1620. [PubMed: 23679870]

(28). Ricard-Blum S; Beraud M; Raynal N; Farndale RW; Ruggiero F Structural Requirements for Heparin/Heparan Sulfate Binding to Type V Collagen. J. Biol. Chem. 2006, 281, 25195–25204. [PubMed: 16815843]

(29). Vanpouille C; Denys A; Carpentier M; Pakula R; Mazurier J; Allain F Octasaccharide Is The Minimal Length Unit Required for Efficient Binding of Cyclophilin B to Heparin And Cell Surface Heparan Sulphate. Biochem. J. 2004, 382 (Pt 2), 733–740. [PubMed: 15109301]

(30). Smith RAA; Murali S; Rai B; Lu X; Lim ZXH; Lee JJL; Nurcombe V; Cool SM Minimum Structural Requirements for BMP-2-Binding of Heparin Oligosaccharides. Biomaterials 2018, 184, 41–55. [PubMed: 30205243]

(31). Slabinski L; Jaroszewski L; Rodrigues AP; Rychlewski L; Wilson IA; Lesley SA; Godzik A The Challenge of Protein Structure Determination-Lessons from Structural Genomics. Protein Sci. 2007, 16, 2472–2482. [PubMed: 17962404]

(32). Li Y; Yu H; Thon V; Chen Y; Muthana MM; Qu J; Hie L; Chen X Donor Substrate Promiscuity of The N-Acetylglucosaminyltransferase Activities of *Pasteurella multocida* Heparosan Synthase 2 (PmHS2) and *Escherichia coli* K5 KfiA. Appl. Microbiol. Biotechnol. 2014, 98, 1127–1134. [PubMed: 23661084]

(33). Lau K; Thon V; Yu H; Ding L; Chen Y; Muthana MM; Wong D; Huang R; Chen X Highly Efficient Chemoenzymatic Synthesis of beta1–4-Linked Galactosides with Promiscuous Bacterial beta1–4-Galactosyltransferases. Chem. Commun. 2010, 46, 6066–6068.

(34). Li Y; Yu H; Chen Y; Lau K; Cai L; Cao H; Tiwari VK; Qu J; Thon V; Wang PG; Chen X Substrate Promiscuity of N-Acetylhexosamine 1-Kinases. Molecules 2011, 16, 6396–6407. [PubMed: 21799473]

(35). Chen Y; Thon V; Li Y; Yu H; Ding L; Lau K; Qu J; Hie L; Chen X One-Pot Three-Enzyme Synthesis of UDP-GlcNAc Derivatives. Chem. Commun. 2011, 47, 10815–10817.

(36). Muthana MM; Qu J; Xue M; Klyuchnik T; Siu A; Li Y; Zhang L; Yu H; Li L; Wang PG; Chen X Improved One-Pot Multienzyme (OPME) Systems for Synthesizing UDP-Uronic Acids And Glucuronides. Chem. Commun. 2015, 51, 4595–4598.

(37). Muthana MM; Qu J; Li Y; Zhang L; Yu H; Ding L; Malekan H; Chen X Efficient One-Pot Multienzyme Synthesis of UDP-Sugars Using A Promiscuous UDP-Sugar Pyrophosphorylase from *Bifidobacterium longum* (BLUSP). Chem. Commun. 2012, 48, 2728–2730.

(38). Zhang C; Griffith BR; Fu Q; Albermann C; Fu X; Lee IK; Li L; Thorson JS Exploiting The Reversibility of Natural Product Glycosyltransferase-Catalyzed Reactions. Science 2006, 313, 1291–1294. [PubMed: 16946071]

(39). Gantt RW; Peltier-Pain P; Cournoyer WJ; Thorson JS Using Simple Donors to Drive The Equilibria of Glycosyltransferase-Catalyzed Reactions. Nat. Chem. Biol. 2011, 7, 685–691. [PubMed: 21857660]

(40). Chandrasekaran EV; Xue J; Xia J; Locke RD; Matta KL; Neelamegham S Reversible Sialylation: Synthesis of Cytidine 5'-Monophospho-N-Acetylneuraminic Acid from Cytidine 5'-Monophosphate with alpha2,3-Sialyl O-Glycan-, Glycolipid-, And Macromolecule-Based Donors Yields Diverse Sialylated Products. Biochemistry 2008, 47, 320–330. [PubMed: 18067323]

(41). Mehr K; Withers SG Mechanisms of The Sialidase And Trans-Sialidase Activities of Bacterial Sialyltransferases from Glycosyltransferase Family 80. Glycobiology 2016, 26, 353–359. [PubMed: 26582604]

(42). McArthur JB; Yu H; Tasnima N; Lee CM; Fisher AJ; Chen X Alpha2–6-Neosialidase: A Sialyltransferase Mutant as A Sialyl Linkage-Specific Sialidase. ACS Chem. Biol. 2018, 13, 1228–1234. [PubMed: 29543427]

(43). Chavaroche AA; van den Broek LA; Boeriu C; Eggink G Synthesis of Heparosan Oligosaccharides by *Pasteurella multocida* PmHS2 Single-Action Tansferases. Appl. Microbiol. Biotechnol. 2012, 95, 1199–1210. [PubMed: 22198719]

(44). Li Y; Xue M; Sheng X; Yu H; Zeng J; Thon V; Chen Y; Muthana MM; Wang PG; Chen X Donor Substrate promiscuity of bacterial beta1–3-N-acetylglucosaminyltransferases and acceptor substrate flexibility of beta1–4-galactosyltransferases. Bioorg. Med. Chem. 2016, 24, 1696–1705. [PubMed: 26968649]

(45). Yu H; Chokhawala H; Karpel R; Yu H; Wu B; Zhang J; Zhang Y; Jia Q; Chen X A Multifunctional *Pasteurella multocida* Sialyltransferase: A Powerful Tool for The Synthesis of Sialoside Libraries. J. Am. Chem. Soc. 2005, 127, 17618–17619. [PubMed: 16351087]

(46). Yang J; Yan R; Roy A; Xu D; Poisson J; Zhang Y The I-TASSER Suite: Protein Structure And Function Prediction. Nat. Meth. 2015, 12, 7–8.

(47). Roy A; Kucukural A; Zhang Y I-TASSER: A Unified Platform for Automated Protein Structure And Function Prediction. Nat. Protoc. 2010, 5, 725–738. [PubMed: 20360767]

(48). Osawa T; Sugiura N; Shimada H; Hirooka R; Tsuji A; Shirakawa T; Fukuyama K; Kimura M; Kimata K; Kakuta Y Crystal Structure of Chondroitin Polymerase from *Escherichia coli* K4. Biochem. Biophys. Res. Commun. 2009, 378, 10–14. [PubMed: 18771653]

(49). Persson K; Ly HD; Dieckelmann M; Wakarchuk WW; Withers SG; Strynadka NC Crystal Structure of The Retaining Galactosyltransferase LgtC from *Neisseria meningitidis* in Complex with Donor And Acceptor Sugar Analogs. Nat. Struct. Biol. 2001, 8, 166–175. [PubMed: 11175908]

(50). Lairson LL; Chiu CP; Ly HD; He S; Wakarchuk WW; Strynadka NC; Withers SG Intermediate Trapping on A Mutant Retaining Alpha-Galactosyltransferase Identifies An Unexpected Aspartate Residue. J. Biol. Chem. 2004, 279, 28339–28344. [PubMed: 15075344]

(51). Gomez H; Polyak I; Thiel W; Lluch JM; Masgrau L Retaining Glycosyltransferase Mechanism Studied by QM/MM Methods: Lipopolysaccharyl-Alpha-1,4-Galactosyltransferase C Transfers Alpha-galactose via An Oxocarbenium Ion-Like Transition State. J. Am. Chem. Soc. 2012, 134, 4743–4752. [PubMed: 22352786]

(52). Jamaluddin H; Tumbale P; Withers SG; Acharya KR; Brew K Conformational Changes Induced by Binding UDP-2F-Galactose to Alpha-1,3 Galactosyltransferase- Implications for Catalysis. J. Mol. Biol. 2007, 369, 1270–1281. [PubMed: 17493636]

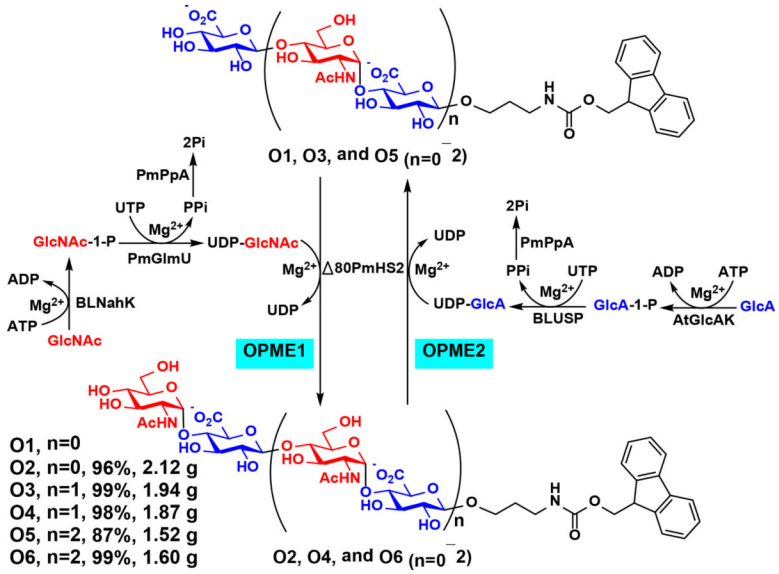

Scheme 1.

Δ80PmHS2-dependent sequential one-pot multienzyme (OPME) synthesis of heparosan oligosaccharides O2–O6.

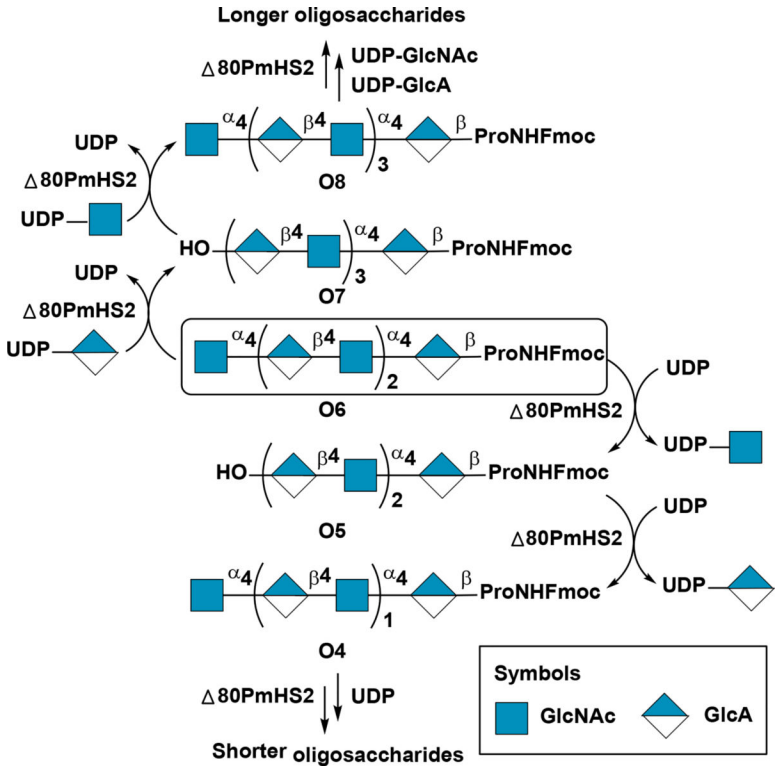

Scheme 2.

Schematic illustration of the chain reactions caused by forward and reverse glycosylation activities of Δ80PmHS2 in the presence of hexasaccharide O6 and UDP.

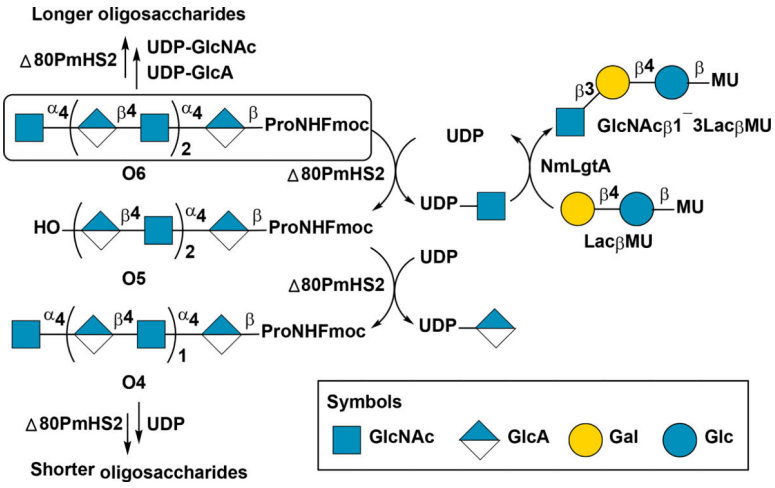

Scheme 3.

Schematic illustration for indirectly detecting UDP-GlcNAc formed in the reverse glycosylation reaction of Δ80PmHS2 in the presence of UDP and hexasaccharide O6 using a coupled enzyme assay with NmLgtA and LacβMU.

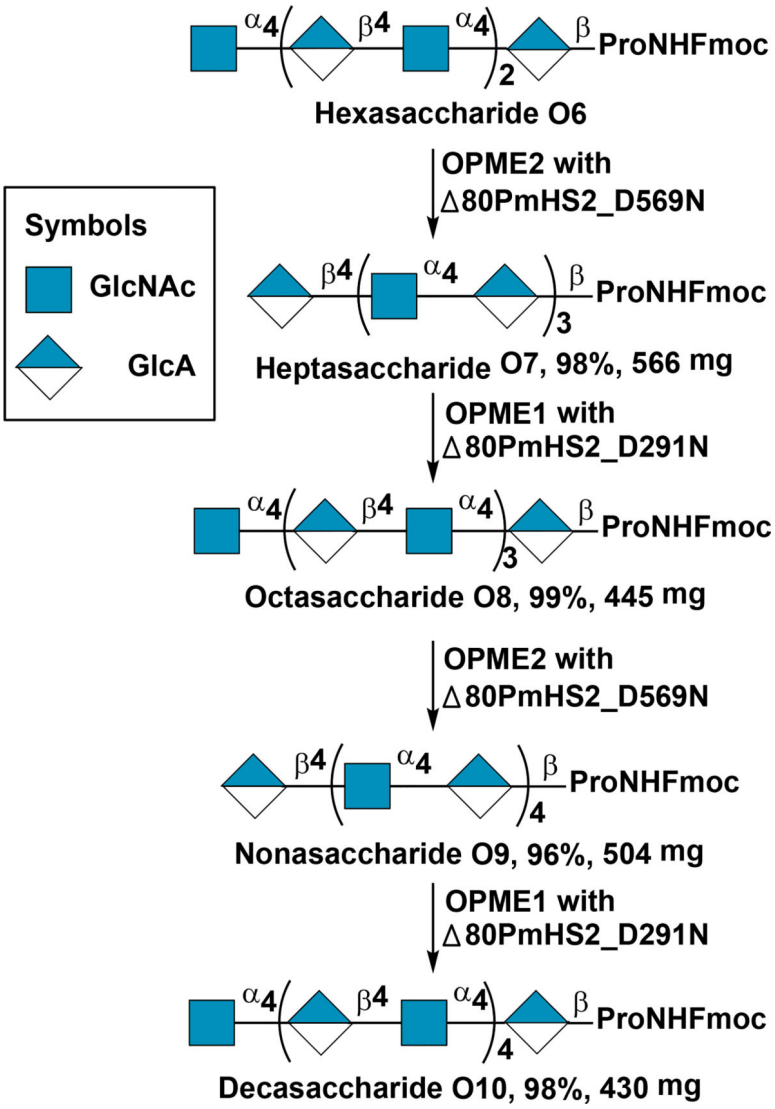

Scheme 4.

Sequential OPME synthesis of heparosan oligosaccharides O7–O10.